Microsystem Technologies (2023) 29:1099–1105
https://doi.org/10.1007/s00542-023-05481-2

TECHNICAL PAPER

Intelligent equipment maintenance and diagnosis method based on VS-Harmogram method

Kun Zhang[1,2] · Ling Shi[3] · Peng Chen[2]

Received: 12 September 2022 / Accepted: 30 May 2023 / Published online: 12 June 2023

Abstract
The intelligent maintenance of rotating machinery is inseparable from the real-time condition detection and fault diagnosis system. The traditional blind source fault diagnosis method has low efficiency and high misdiagnosis rate, so this paper introduces the VS-Harmogram method with prior parameters. First, the Fourier spectrum should be re-cut by power spectral density and the information in each frequency band can be sequentially extracted. Secondly, the window width of power spectral density is gradually increased to expand the variability of the sweep frequency. Finally, the harmonic spectral kurtosis of each component should be calculated using the prior parameters of the rotating equipment. A variable spectral segmentation Harmogram (VS-Harmogram) with multiple sets of boundaries would be constructed. The validity of the method can be verified by using the fault signals of rolling bearings in rotating equipment.

1 Introduction

The maintenance and diagnosis of industrial equipment requires the support of advanced theories and algorithms, but traditional digital signal analysis methods cannot adapt to complex new equipment (Wang et al. 2017). Healthy bearings are the basis for the normal operation of equipment, and bearings that are easily damaged and fail are also one of the biggest hidden dangers that lead to equipment failure (Hu et al. 2016). In order to adaptively extract fault features in vibration signals of rotating machinery rolling bearings, scholars gradually turn the recognition objects from time-domain features to frequency-domain features (Zhang et al. 2021; Li et al. 2022).

Traditional fault diagnosis methods rely on the performance of sensors, and Bapi Debnath (2020) designed a novel piezoelectric sensor to detect faults in small rolling bearings. Yu et al. (2014) introduced the relative vibration analysis of PMSM based on fuzzy mathematics. For wireless multi-channel signals, Chen et al. (2021) uses backpropagation neural network and wavelet packet algorithm for fusion processing to extract more obvious features. Antoni (2007) first gave formal mathematical definition of spectral kurtosis and proved that it is sensitive to impulse characteristics in noisy non-stationary signals. SK is applied to the Kurtogram to suppress interference and extract fault information. The modal decomposition from the frequency domain and screening of signal features provides more ideas for subsequent research (Tang 2021; Zhong et al. 2021; Zhang et al. 2022). Moshrefzadeh and Fasana (2018) used the Maximal overlap discrete wavelet packet transform to replace the filter used by Kurtogram to obtain a more accurate envelope spectrum. The fixed frame adopted by this type of method may not be able to adapt to the changing system, which is the main direction of this paper.

In this paper, a variable spectral segmentation framework replaces the average spectral segmentation framework. We construct the outline of the filtering framework by changing the window width of the power spectral

✉ Kun Zhang
zkun212@163.com

Ling Shi
shiling689@163.com

Peng Chen
chen@bio.mie-u.ac.jp

[1] The Key Laboratory of Advanced Manufacturing Technology, Beijing University of Technology, Beijing 100124, China

[2] Graduate School of Environmental Science and Technology, Mie University, Tsu 514-0001, Japan

[3] The Laboratory of Automatic detection and Fault Diagnosis, Harbin University of Science and Technology, Harbin 150080, China

density (PSD) to obtain different minimum point distributions. The harmonic spectral kurtosis of each component should be calculated using the prior parameters of the rolling bearings. A variable spectral segmentation Harmogram (VS-Harmogram) would be constructed. The validity of the method can be verified by using the fault signals of rolling bearings in rotating equipment. The paper is organized as follows. In Sect. 2, variable spectral segmentation Harmogram are introduced. The simulation signals are given in Sect. 3 to obtain the optimal frequency band. The data of Case Western Reserve University are used to verify the effectiveness of the proposed method in Sect. 5.

2 Variable spectral Harmogram

In this paper, a variable spectral segmentation Harmogram is designed to diagnose faults in industrial equipment to assist maintenance. The steps can be described as follows:

(i) Continuously increase the window width and calculate the PSD of each round based on Welch's method.
(ii) Define the minimum value of the PSD as the boundary, obtain the components of each frequency band.
(iii) Calculate the harmonic spectral kurtosis of each independent component.
(iv) Construct VS-Harmogram using all boundary groups and harmonic spectral kurtosis. Extract the component represented by the largest harmonic spectral kurtosis to diagnose faults.

2.1 PSD based mode decomposition method

Different levels of PSD can be obtained according to different window widths. Low-level PSD correspond to rough spectral fluctuation trends, and high-level PSD correspond to complex spectral energies. PSD actually represents the distribution of power with frequency. The average power of signal y(t)can be described as (Krapf et al. 2018):

$$P = \lim_{T\to\infty} \frac{1}{2T} \int_{-T}^{T} y(t)^2 dt \tag{1}$$

Suppose the Fourier transform of the signal in the interval [0, T] is:

$$\widehat{y}_T(f) = \frac{1}{\sqrt{T}} \int_{0}^{T} y(t) e^{-i2\pi ft} dt \tag{2}$$

Power spectral density can be defined as:

$$S_{yy}(f) = \lim_{T\to\infty} E\left[|\widehat{y}_T(f)|^2\right] \tag{3}$$

Since PSD is positive and has a correlation with Fourier spectrum, this paper calculates the minimum point of the PSD of each level to determine the division method of the Fourier spectrum.

2.2 Harmonic spectral kurtosis

Faulty bearing signals in rotating machinery often have distinctive characteristics. There are periodic pulses in the time domain waveform. In the Fourier spectrum there are impulse bands containing fixed sidebands. The fault characteristic frequencies and their harmonics are present in the Hilbert envelope spectrum. To quantify the fault feature information in the Hilbert envelope spectrum, we design the harmonic spectral kurtosis index (Zhang et al. 2021).

Non-stationary signal and its frequency counterpart is:

$$y(t) = \int_{-\infty}^{t} g(t, t-\tau) x(\tau) d_\tau \tag{4}$$

$$y(t) = \int_{-\infty}^{+\infty} e^{j2\pi ft} P(t,f) d_{X(f)} \tag{5}$$

where $P(t,f)$ is the complex envelope or complex demodulate of the signal at f.

The randomized cyclostationary processes is:

$$g(t,s) = g(t+T,s) = \sum_k g_k(s) e^{j2\pi kt/T} \tag{6}$$

$$g_0(t,\Delta t) = \sum_n g_n(nt) e^{j2\pi nt/T} \tag{7}$$

$g_0(t,\Delta t)$ have periodic instantaneous pulses in $(-\Delta t, \Delta t)$ near nt of $g(t,s)$ which is shown in Fig. 1.

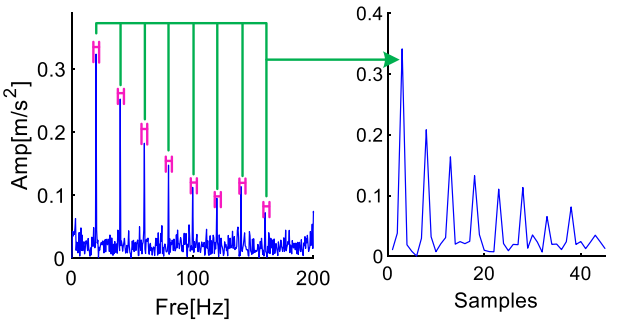

(a) Envelope spectrum of bearing outer ring fault data (b) Instantaneous moment of characteristic

Fig. 1 Schematic diagram of IMC

The 2n-order harmonic instantaneous moment can be defined as:

$$S_{2HY}(t,f) = E\left\{\left|P_n(t,f)d_{X(f)}\right|^2\right\}/d_f = |P_n(t,f)|^2 \cdot S_{2X} \quad (8)$$

The spectral moments of $S_{2HY}(t,f)$ is:

$$S_{2HY}(f) = E\{S_{2HY}(t,f)\} = E\left\{|P_n(t,f)|^2\right\} \cdot S_{2X} \quad (9)$$

2n-order harmonic average moment can be defined as:

$$\langle S_{2HY}(t,f)\rangle_t = \lim_{T\to\infty} 1/T \int_{-T/2}^{T/2} S_{2HY}(t,f)d_t \quad (10)$$

The normalized fourth-order harmonic spectral moment is:

$$C_{4HY}(f) = S_{4HY}(f); \quad f \neq 0 \quad (11)$$

Harmonic Spectral Kurtosis (HSK) is defined as the energy-normalised fourth-order harmonic spectral cumulant:

$$HSK_Y(f) = \frac{C_{4HY}(f)}{S_{2Y}^2(f)} = \frac{S_{4HY}(f)}{S_{2Y}^2(f)}; \quad f \neq 0 \quad (12)$$

3 Simulation signal verification

Define the non-stationary periodic impulse signal with white Gaussian noise, the first is the periodic impulse signal; the second is the modulation signal.

$$\begin{cases} s_{c1} = \sum_{i=1}^{20} 9e^{-g\times 2\pi f_n^i t} \times \sin\left(2\pi f_n^i t \times \sqrt{1-g^2}\right) \\ s_{c2} = 5\cos(100\pi t) \times \sin(6000\pi t + \sin(200\pi t)) \\ s_1 = s_{c1} + s_{c2} + \zeta \end{cases} \quad (13)$$

where $f_n = 3000$Hz, damping coefficient $g = 0.07$, pulses period $T = 0.01$s, noise $\zeta = \mathrm{SNR}(5dB)$. The waveform and spectrum of the signal are shown in Fig. 2.

It can be found from Fig. 2d that there are two components and a lot of noise in the Fourier spectrum. The method proposed in this paper is used to calculate the PSD of different levels of the signal and calculate their minimum points. Then a tower frame diagram can be designed. Fill the calculated HSK of each frequency band into the frame, and the proposed VS-Harmogram is constructed, as shown in Fig. 3.

Extract the frequency band with the largest HSK and display the waveform and envelope spectrum of component-A in Fig. 4. It can be found that there are a large number of periodic pulses in the component, and the envelope spectrum contains periodic pulse characteristic frequencies and harmonics. Therefore, the proposed method can accurately extract information containing such features from the signal.

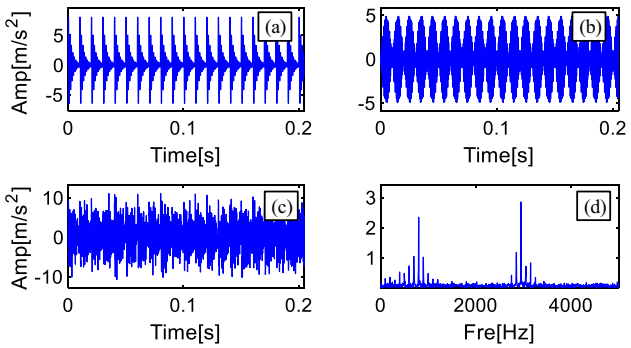

Fig. 2 Simulation signal and its spectrum

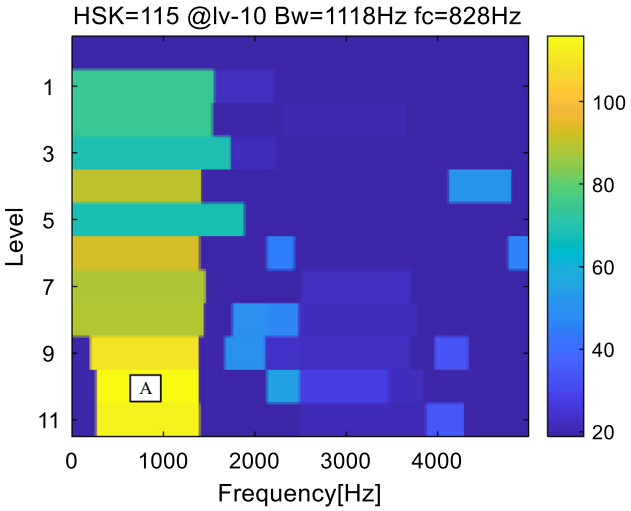

Fig. 3 VS-Harmogram

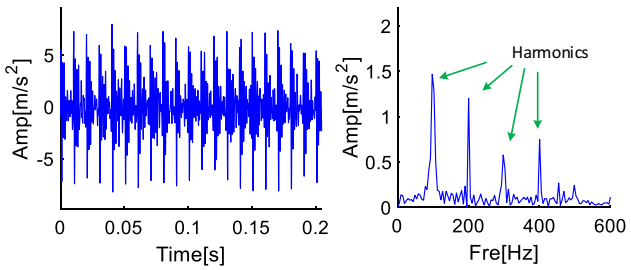

(a) Component A (b) Envelope spectrum

Fig. 4 Extracted component-A and envelope spectrum

4 Application

This paper uses the Case Western Reserve University (CWRU) Bearing Test Rig that has a 2 HP Reliance motor, a torque sensor and a dynamometer which is shown in

Fig. 5. The drive end bearing (deep groove ball bearing) is type 6205-2RS JEM SKF. Motor speed is 1797 rpm. Bearing specifications are shown in Table 1.

The width of the faulty bearing outer ring injury is 0.1778 mm and the depth is 0.2794 mm. After calculation, the fault characteristic frequency of the outer ring of the bearing is 107.305 Hz, and the period is 0.00932 s. Figure 2 shows the signal and its spectrum.

Bearing fault information may be concentrated in a certain frequency band, which requires the method proposed in this paper to find. The VS-Harmogram-based algorithm designed 7 levels of PSD distributions and calculated their respective boundaries sequentially. The final tower distribution diagram is shown in Fig. 6.

The component-B with the largest HSK is located at Level-2, which corresponds to the region of the spectrum with the largest amplitude. Extract this component and display its waveform with the Hilbert envelope spectrum, which can be seen in Fig. 7.

The envelope spectrum contains the fault characteristic frequency of the outer ring of the bearing and its harmonics. Therefore, we judge that the bearing outer ring is damaged, and the proposed method can be applied to bearing fault diagnosis.

A classical spectral kurtosis-based algorithm called Kurtogram is presented as a comparison target in this paper. Kurtogram is characterized by fast calculation speed, and its theoretical basis is the multi-level average division of the spectrum. These characteristics are correspondingly different from those in this paper, so it is very suitable as a reference frame to verify the advantages of the algorithm proposed in this paper. Figure 8 is the processing result of Kurtogram. This figure uses a method based on short-time Fourier transform and spectral kurtosis to construct a tower diagram. The calculation speed of tower diagram obtained by this method is very fast, but the accuracy is relatively low. Important information in the signal may not be recognized. We can find the frequency band with relatively large kurtosis value from the figure. There is a higher amplitude at 1875 Hz. At the same time, there is also a higher amplitude at 5500 Hz. However, the algorithm eventually extracted the information at 1875 Hz.

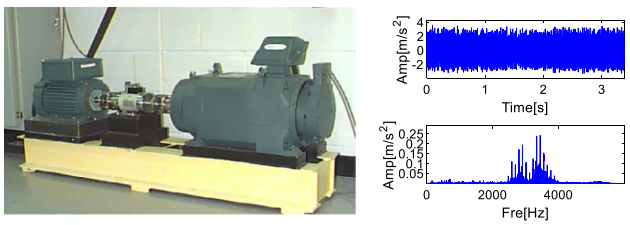

Fig. 5 CWRU bearing test rig and the outer ring vibration signal

If we extract the information around 1875 Hz, the waveform and envelope spectrum of the signal in this frequency band can be shown in Fig. 9. Although double and triple harmonics exist in the envelope spectrum, there are no characteristic frequencies, and their amplitudes have no greater advantage compared to VS-Harmogram.

The above experiments have verified that this method is effective for bearing outer ring fault diagnosis. Therefore, it is also necessary to test the bearing inner ring fault and verify the effectiveness of this method. This section continues to use the data from Case Western Reserve University. For bearing inner ring fault data, we used inner ring damage data with the same sampling frequency/installation location/damage size. The specific parameters of the bearing can refer to Table 1. First, we need to display the waveform and frequency spectrum of the data, as shown in Fig. 10.

The signal length shown in Fig. 10 is about 3.5 s, which contains a lot of pulses and noise. There are four center frequencies in the spectrum that contain sidebands around them. The distribution of these center frequencies is not regular, so evenly splitting the spectrum cannot explain its rationality theoretically. The frequency band obtained by the VS-Harmogram proposed in this paper has strong noise resistance and is not easily disturbed by the minimum point generated by noise. Figure 11 shows the characteristics of the algorithm.

We can find from Fig. 10 that there are large peaks in the frequency bands [0–1000 Hz], [1000–2000 Hz], [2000–3000 Hz], [3000–4500 Hz]. In Fig. 11, the boundary distribution obtained after VS-Harmogram calculation can separate these frequency bands. When the levels are 6–9, the results of spectral segmentation are almost the same, which means that the algorithm has low error tolerance. The frequency band with high harmonic spectrum kurtosis is located near 2600 Hz, and the bandwidth is about 960 Hz. Extracting this component, we can find the characteristic frequency and its harmonics of the bearing inner ring fault from Fig. 12, which means that VS-Harmogram can successfully extract the bearing inner/outer ring fault.

When calculating the bearing inner ring fault data, we used the aforementioned Kurtogram constructed based on the short-time Fourier transform. Likewise, the signal was averaged 11 times. The spectral kurtosis of the signal in each frequency band is calculated. Finally, the part with the center frequency of 4500 Hz obtained the largest kurtosis value (Fig. 13).

After extract the component around 4500 Hz, its envelope spectrum are shown in Fig. 14. No characteristic frequencies or harmonics exist in the envelope spectrum. It is difficult to judge the fault of the signal.

Table 1 Bearing specifications (mm)

Inside diameter	Outer diameter	Width	Ball diameter	Pitch diameter
25	52	15	7.94	39.04

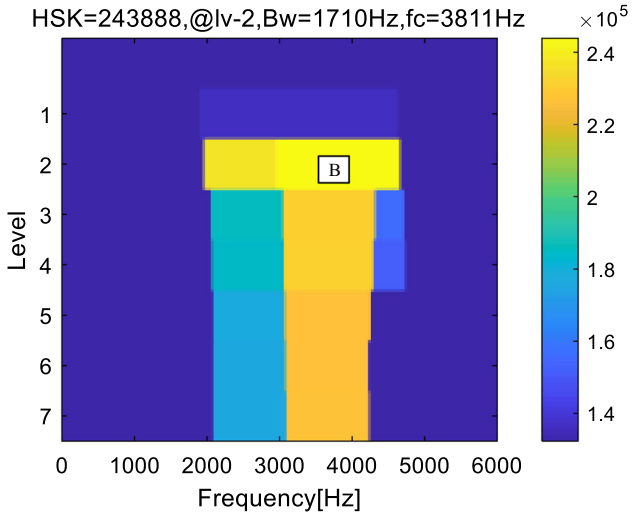

Fig. 6 VS-Harmogram

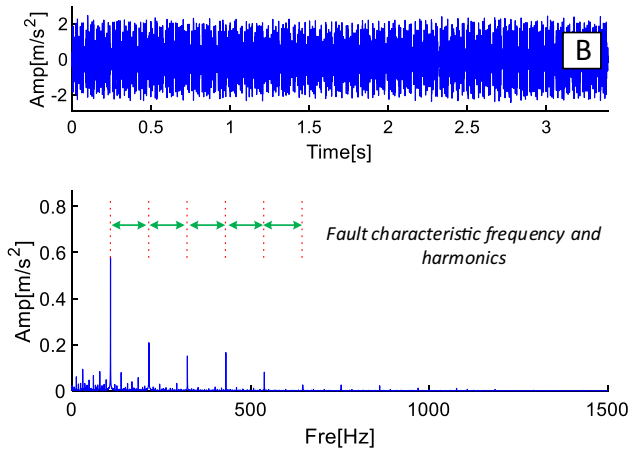

Fig. 7 Extracted component-B and envelope spectrum

5 Conclusion

This paper proposes a VS-Harmogram method based on spectral segmentation framework and harmonic spectral kurtosis. Different windows are used to calculate different levels of power spectral density to construct a variable spectral partitioning framework. Harmonic spectral kurtosis that identifies periodic pulse information from the envelope spectrum is used to extract bearing fault information. Simulation and experimental data verify that the proposed method is suitable for bearing fault diagnosis in industrial equipment.

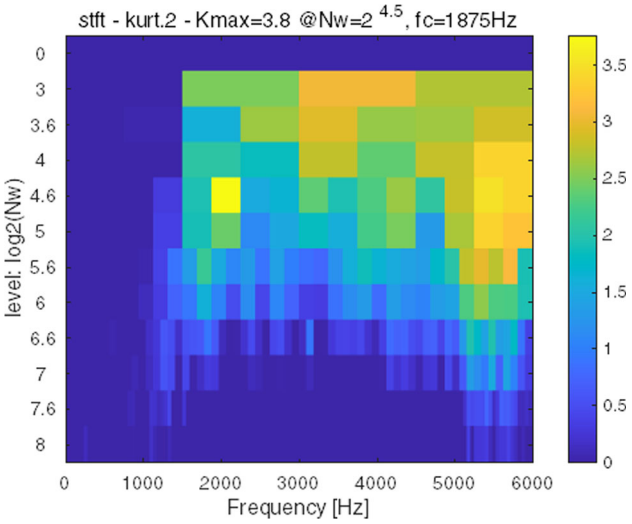

Fig. 8 Kurtogram

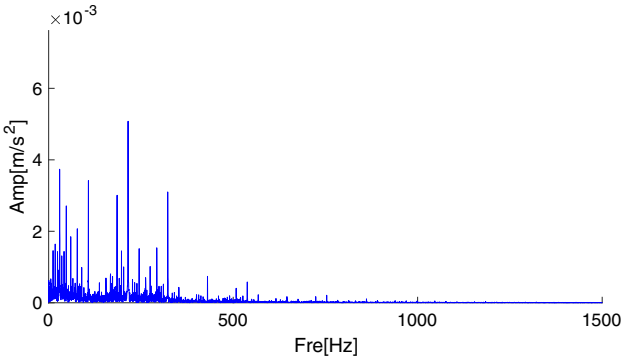

Fig. 9 Extracted component by Kurtogram and the envelope spectrum

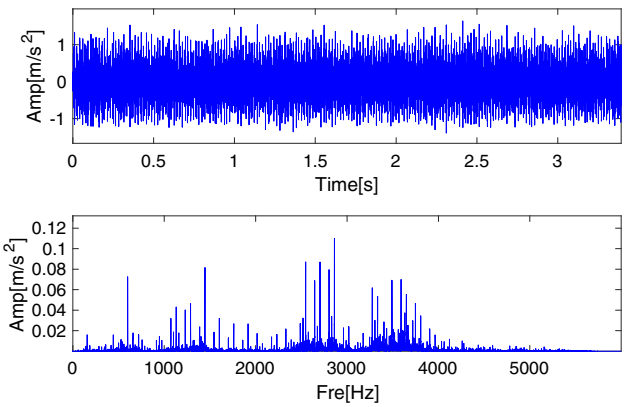

Fig. 10 CWRU bearing inner ring vibration signal

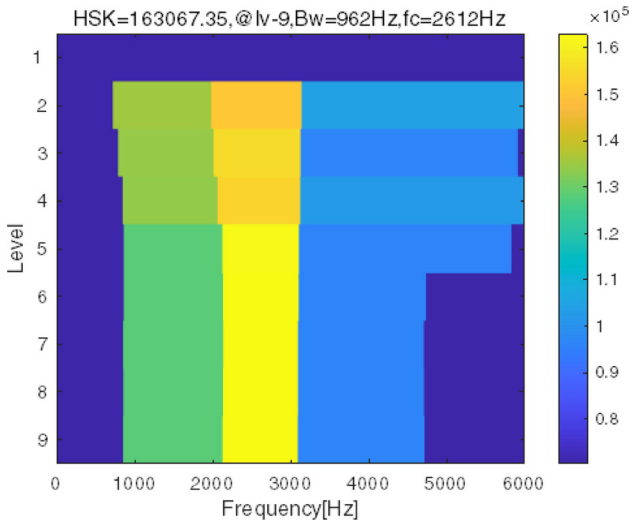

Fig. 11 VS-Harmogram

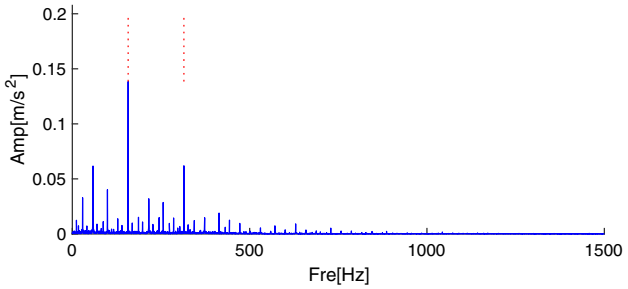

Fig. 12 The envelope spectrum of extracted component

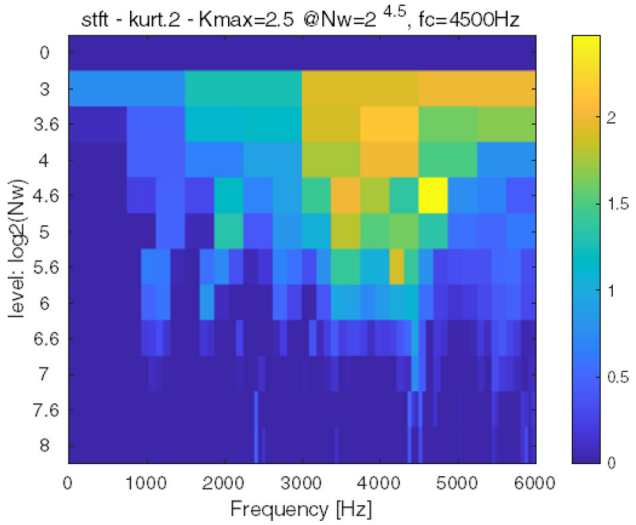

Fig. 13 Kurtogram

6 Discussion

Although this paper has carried out post-processing for the collected data, its disadvantage is that the calculation time is slow and only one set of data can be processed. At present, sensors are being researched by more scholars and institutions and have been more fully developed. Sensors with high sampling frequency and precision will obtain rich data. It is necessary to put forward higher requirements for the algorithm in this case. The core of the algorithm is to process the frequency domain of the signal. If multiple sets of data collected by different sensors are fused in the frequency domain, the efficiency of the algorithm will be improved.

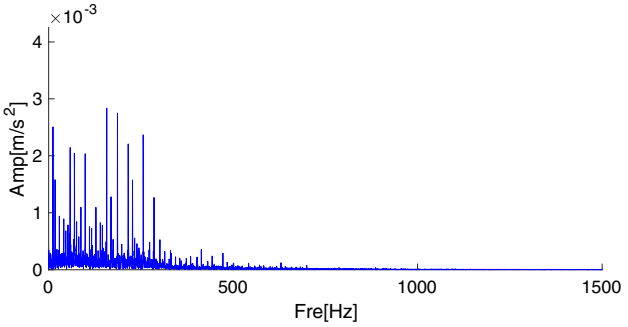

Fig. 14 The envelope spectrum of the extracted component by Kurtogram

Acknowledgements The work was supported by the National Natural Science Foundation of China (Grant Nos. 51775005). The authors would like to thank the editors and reviewers for their valuable comments and constructive suggestions.

Data availability This manuscript adopts a publicly available dataset: https://engineering.case.edu/bearingdatacenter

References

Antoni J (2007) Fast computation of the kurtogram for the detection of transient faults. Mech Syst Signal Process 21(1):108–124

Chen Q, Hu Y, Xia J (2021) Data fusion of wireless sensor network for prognosis and diagnosis of mechanical systems. Microsyst Technol 27:1187–1199

Debnath B, Kumar R (2020) A new Tapered-L shaped springs based MEMS piezoelectric vibration energy harvester designed for small rolling bearing fault detection. Microsyst Technol 26:2407–2422

Hu Y, Li F, Li H (2016) An enhanced empirical wavelet transform for noisy and non-stationary signal processing. Digit Signal Process 60:220–229

Krapf D, Marinari E, Metzler R, Oshanin G, Xu X, Squarcini A (2018) Power spectral density of a single brownian trajectory: what one can and cannot learn from it. New J Phys 20:023029

Li X, Shao H, Lu S, Xiang J, Cai B (2022) Highly-efficient fault diagnosis of rotating machinery under time-varying speeds using LSISMM and small infrared thermal images. IEEE Trans Syst Man Cybern: Syst. https://doi.org/10.1109/TSMC.2022.3151185

Moshrefzadeh A, Fasana A (2018) The Autogram: an effective approach for selecting the optimal demodulation band in rolling element bearings diagnosis. Mech Syst Signal Process 105:294–318

Tang H, Liao Z, Chen P (2021) A robust deep learning network for low-speed machinery fault diagnosis based on multi-kernel and

RPCA. IEEE-ASME Trans Mech 27(3):1522–1532. https://doi.org/10.1109/TMECH.2021.3084956
Wang D, Zhao Y, Yi C (2017) Sparsity guided empirical wavelet transform for fault diagnosis of rolling element bearings. Mech Syst Signal Process 101:292–308
Yu Y, Bi C, Jiang Q (2014) Vibration study and classification of rotor faults in PM synchronous motor. Microsyst Technol 20:1653–1659
Zhang K, Xu Y, Liao Z, Song L, Chen P (2021) A novel fast Entrogram and its applications in rolling bearing fault diagnosis. Mech Syst Signal Process 154(1):107582
Zhang K, Chen P, Yang M (2022) The Harmogram: a periodic impulses detection method and its application in bearing fault diagnosis. Mech Syst Signal Process 165:108374
Zhong J, Bi X, Shu Q, Zhang D, Li X (2021) An improved wavelet spectrum segmentation algorithm based on spectral kurtogram for denoising partial discharge signals. IEEE Trans Instrum Meas 70:1–8